*Korean J. Chem. Eng.*, **29**(3), 356-361 (2012)
DOI: 10.1007/s11814-011-0291-2

# Effect of an electrodeposited $TiO_2$ blocking layer on efficiency improvement of dye-sensitized solar cell

**Kang-Il Jang, Eunpyo Hong, and Jung Hyeun Kim†**

Department of Chemical Engineering, University of Seoul, Seoul 130-743, Korea
(*Received 24 Ocotber 2011 • accepted 17 November 2011*)

**Abstract**–A $TiO_2$ blocking layer in DSSC provides good adhesion between the fluorinated tin oxide (FTO) and an active $TiO_2$ layer, and represses the electron back transport between electrolyte and FTO by blocking direct contact. In addition, it offers a more uniform layer than bare FTO glass. In this study, a dense $TiO_2$ layer is prepared by electrodeposition technique onto an FTO substrate, and it is further used for efficiency measurement of dye-sensitized solar cell (DSSC). The thickness of $TiO_2$ blocking layers is controlled by applied voltage and deposition time. The morphology and crystalline structure of $TiO_2$ blocking layers are characterized by scanning electron microscopy (SEM), atomic force microscopy (AFM) and X-ray diffraction (XRD). The effect of thickness of $TiO_2$ blocking layers on transmittance is also examined by UV-vis spectrophotometer. For the best performance of the cell efficiency, the optimum blocking layer thickness is about 450 nm fabricated at 0.7 V for 20 min. The conversion efficiency from the DSSC including the optimum blocking layer is 59.34% improved compared to the reference cell from 2.41% to 3.84%. It demonstrates that the electrodeposition is a useful method to produce $TiO_2$ blocking layer for DSSC applications.

Key words: DSSC, Blocking Layer, Electrodeposition, $TiO_2$ Film

## INTRODUCTION

Production of energy from fossil materials has polluted the environment. The conversion of solar radiation to electricity has become more and more important, because sunlight is a clean and limitless energy source compared to the traditional fossil energy source [1-3]. DSSC, a device that converts sunlight into electricity based on dye-sensitized $TiO_2$ nanocrystalline film, has attracted considerable attention due to its low cost and easy process. However, DSSC has a problem of relatively low conversion efficiency compared to other silicon-based solar cells. Some hot issues to increase the efficiency are the suitable structure of porous $TiO_2$ film at nanoscale in order to increase the amount of dye adsorption and an effective model to expedite the transport of electrons [2,4].

In DSSC, an electron transfer cycle is completed by the following process. The electrons excited from dye are transferred through the conducting band of $TiO_2$ nanocrystallite and FTO electrode, step by step [5]. The dye is regenerated by electron donation from the redox system of the electrolyte, such as the iodide/triiodide ($I^-/I_3^-$) couple. The iodide is recovered by reduction of triiodide on the platinum layer of the counter electrode. Among the interfaces described previously, serious recombination of electrons can be conducted between the interface of $TiO_2$/FTO. The electron transfer on the FTO is intercepted by reduction of the electrolyte penetrated onto the electrode. Thus, considerable attention has been focused on reducing electron recombination at the interface between FTO substrate and electrolyte. Previous investigations have demonstrated that it is effective to introduce a compact and thin $TiO_2$ blocking layer onto the transparent conducting glass substrate [6-9]. The schematic on the effect of the blocking layer is shown in Fig. 1. Various preparation methods for the blocking layer have been reported, such as sputtering [10,11], sol-gel [12,13], spray-coating [14,15], spin coating [16], and dip coating [17] techniques. However, these methods suffer from high cost and difficult process control, as well as other problems.

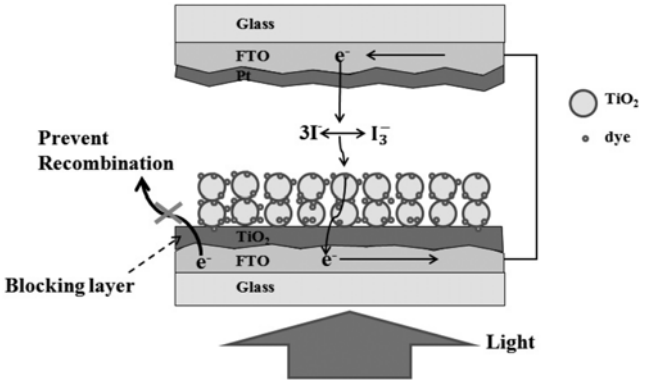


**Fig. 1. Schematic view of the DSSC including a blocking layer for preventing electron recombination.**

In this study, which is targeted to overcome the faults of these methods, the electrodeposition is proposed with its simple process and easy control [18-20]. Several researches have tried to apply the electrodeposition to produce a densely packed blocking layer [21,22]. However, those reports are limited to just mentioning without further specific investigation. Therefore, more detailed researches on the formation of the blocking layer are required. We systematically examine the effect of the experimental parameters such as deposition time and applied voltage on the formation of the blocking layer and investigate the optimal thickness of $TiO_2$ blocking layer to apply for DSSC by controlling voltage and deposition time.

†To whom correspondence should be addressed.
E-mail: jhkimad@uos.ac.kr

## EXPERIMENTAL

### 1. Materials

$TiCl_3$ solution of 20 weight percentage was purchased from Alfa Aesar Co. Ltd. (USA) for electrodeposition. The colloidal $TiO_2$ paste for doctor blade was obtained by adding 0.375 g polyethylene oxide (PEO, Sigma-Aldrich), 1.5 g $TiO_2$ particles (P25, Degussa) and 0.3 ml Triton X-100 (Sigma-Aldrich) into 20 ml mixed solution of deionized (DI) water and ethanol (50 : 50 ratio). The solution was stirred for 24 h and then kept at room temperature for further use. $H_2PtCl_6$ (Sigma-Aldrich), N719 (Solaronix), $I^-/I_3^-$ electrolyte (HC-DII, TG-energy) were also used for cell fabrications. FTO conductive glass of 18 $\Omega/cm^2$ was used as substrates.

### 2. Electrodeposition of a $TiO_2$ Blocking Layer on a FTO Substrate

Before electrodeposition, the FTO glass was dipped in a solution of ethanol and acetone (50 : 50 ratio), and it was thoroughly cleaned with ultrasonication in DI water. For preparation of $TiO_2$ blocking layer, 16 vol% of $TiCl_3$ electrolyte solution was prepared by diluting with DI water, and then pH of the solution was adjusted to 2.1-2.2 to increase deposition efficiency as reported elsewhere [23]. A schematic diagram of the electrodeposition system is shown in Fig. 2. Three-electrode electrochemical cells were equipped with a Pt-mesh counter electrode, an Ag/AgCl reference electrode, and a FTO conductive glass (1.5×1.5 $cm^2$) working electrode. Working voltage ranged from 0.1 V to 1.0 V using a potentiostat (Iviumstat, Netherland) for various deposition time periods. After the electrodeposition, the substrates were washed with ethanol and sintered for 30 min at 450 °C.

### 3. Fabrication of DSSC

The $TiO_2$ paste was coated by a doctor blade method on the electrodeposited blocking layer, and it was sintered at 450 °C for 30 min. The thickness of the resulting layer was measured to approximately 17 μm. The active area of the prepared mesoporous $TiO_2$ electrode was 25 $mm^2$ (5 mm×5 mm). Dye adsorption was carried out by dipping the $TiO_2$ electrode in dye solution at room temperature for 24 h. The working electrode was then washed, dried, and used for fabrication of DSSCs. The counter electrodes were prepared by placing a few drops of 0.007 M $H_2PtCl_6$ isopropanol solution on FTO substrates and by sintering at 450 °C for 30 min. The counter electrode was assembled with the dye adsorbed $TiO_2$ working electrode with Surlyn resin (Peccell-Technologies) by heat treatment (90 °C). Finally, the electrolyte was filled to the internal space between two electrodes for electrical measurements.

### 4. Measurements

X-ray diffraction (XRD, D/MAX 2500, Rigaku, Japan) patterns were measured for crystalline structure analysis of $TiO_2$ blocking layers using Cu K$\alpha$ radiation. Scanning electron microscope (SEM, SUPRA 55VP, Germany) and atomic force microscope (AFM, Digital Instrument Nanoscope Multimode Iva, USA) were employed to inspect surface morphologies and thicknesses of the $TiO_2$ blocking layers. A UV-vis spectrophotometer (S-4100, Scinco, Korea) was used for measuring the transmittance of various thicknesses of the $TiO_2$ blocking layers. Finally, the open-circuit voltage $V_{oc}$ (V), short-circuit current density $J_{sc}$ (mW/$cm^2$), fill factor (%) and energy conversion efficiency (%) of DSSCs were measured using a solar simulator (PEC-L11, Japan) and a potentiostat. The light source was a 100 W Xe lamp with light density of AM 1.5 (100 mW/$cm^2$).

## RESULTS AND DISCUSSION

### 1. XRD Analysis

Fig. 3 shows XRD patterns of the electrodeposited $TiO_2$ films formed at various voltages from 0.1 V to 1.0 V for different time periods. The characteristic peaks of all the $TiO_2$ films consist of mostly anatase crystalline phase mixed with some extent of rutile phase. The peak at $2\theta$=25.4 becomes sharp as voltage is increased, which means that the grain size of anatase crystalline $TiO_2$ phase increases. The mean grain size of the crystalline phase can be calculated using Scherrer's equation [24]: $t=0.9\lambda/(\beta\cos\theta)$, where $\lambda$ is the X-ray wavelength 1.54056 (Å), $\beta$ is the full width at half maximum (FWHM) of peaks, and $\theta$ is the Bragg angle. The calculated grain size was grown to about 15 nm for the thickest film, and good crystalline structure of $TiO_2$ film was generated on FTO substrate by electrodeposition.

### 2. SEM Analysis

Fig. 4 shows the SEM images of surface structures of the $TiO_2$ films on FTO substrate fabricated at various applied voltages (0.5 V, 0.7 V, 0.9 V) for various deposition times (5 min, 10 min, 15 min).

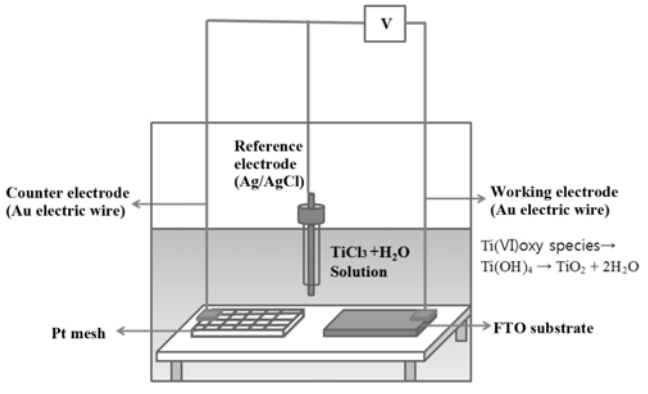


**Fig. 2. Schematic diagram of the electrodeposition cell system with three-electrodes.**

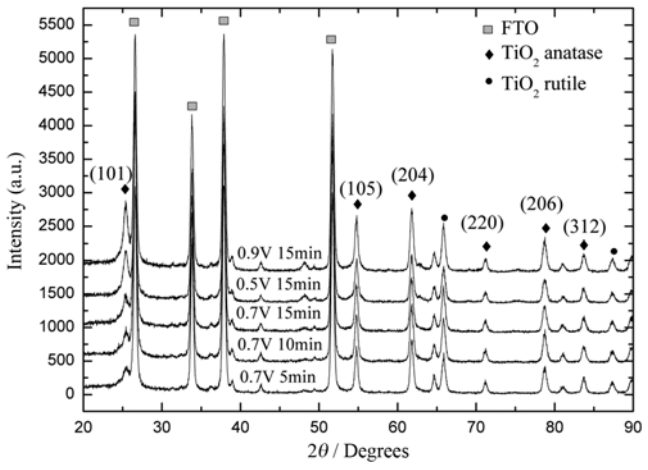


**Fig. 3. XRD patterns of the $TiO_2$ blocking layers electrodeposited at various applied voltages and deposition times.**

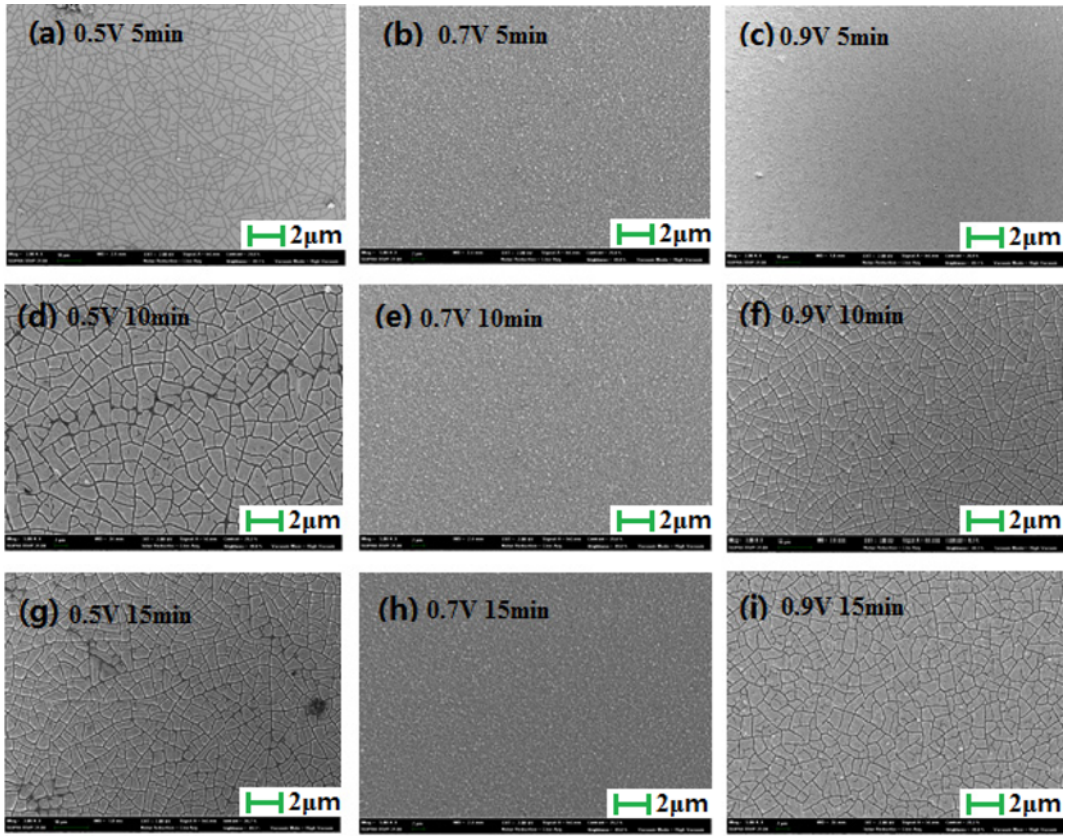


**Fig. 4. SEM images showing variation of surface morphologies formed at various applied voltages and deposition times.**

From the morphologies, uniform surface structure with no cracks was obtained at the applied voltage of 0.7 V in Fig. 4(b), (e), and (h). It demonstrates that there is an optimal voltage condition for film fabrication by electrodeposition method. Two competitive crystal growth mechanisms are reported [25] by electrodeposition reaction, and these are parallel or perpendicular directions to the FTO substrate. For example, applied voltage other than the optimum value produces non-uniform film structure due to the unequal crystal growth in parallel and perpendicular directions. The cracks are clearly seen on the $TiO_2$ films formed at 0.5 V and 0.9 V for all the reaction cases. Therefore, finding an optimum voltage condition for electrodeposition reaction is important for further investigations of DSSC efficiency measurements using the films as blocking layers.

The film thicknesses of $TiO_2$ blocking layers on FTO substrates were also measured by SEM, and three example pictures are shown in Fig. 5. The film thickness increases with increasing applied voltage and with increasing deposition time. For instance, the film thickness increased from 194.1 nm to 247.1 nm as the voltage was increased from 0.6 V to 1.0 V, and it increased from 247.1 nm to 458.8 nm as the depositing time was increased from 5 to 10 min. Film thicknesses measured from all our experimental conditions are shown in Fig. 6, which shows linear increment with applied voltage and deposition time. However, one should be cautious of using high voltage for electrodeposition because it can lead to fall-off problems of the formed particles due to the excessive deposition speed of particles [26].

## 3. UV-vis Spectrophotometer Analysis

The light transmittance is highly dependent on the thickness of films, and it is an important parameter for DSSC applications. As explained above, thickness of the $TiO_2$ blocking layer increases with applied voltage and deposition time. Fig. 7 shows UV-vis transmittance spectra of the $TiO_2$ blocking layers prepared by electrodeposition at 0.7 V for various deposition times including a bare FTO substrate as a reference. As expected, the light transmittance decreased with increasing thickness because light is more absorbed and reflected in thicker film. Through the visible wavelength region, the transmittance decreases gradually until a deposition time of 20 min, but it drops abruptly at 30 min of deposition time. Generally, the N719 dye has good light absorbance at visible light; thus the collection of enough light is expected for the high energy conversion efficiency. Clearly, the light conversion efficiency of DSSC can be affected by the transmittance reduction, for example, around at 480 nm from 42.4% (20 min) to 12.4% (30 min). It will be further discussed in the following cell efficiency section.

## 4. AFM Analysis

The surface morphologies of (a) electrodeposited blocking layer and (b) bare FTO glass were investigated by AFM as shown in Fig. 8. To quantitatively determine the surface roughness, the roughness factor (Ra) of each film was measured. The Ra value on the electrodeposited blocking layer was about 59 nm, but it was about 174 nm from the bare FTO glass. This demonstrates that the electrodeposited $TiO_2$ layer provides much smoother and more uniform surface than the bare FTO substrate case, and it further offers excellent surface flatness after the $TiO_2$ particle layer from the doctor blade process. In addition, the flatness of this $TiO_2$ blocking layer might possess a good characteristic for preventing electron recom-

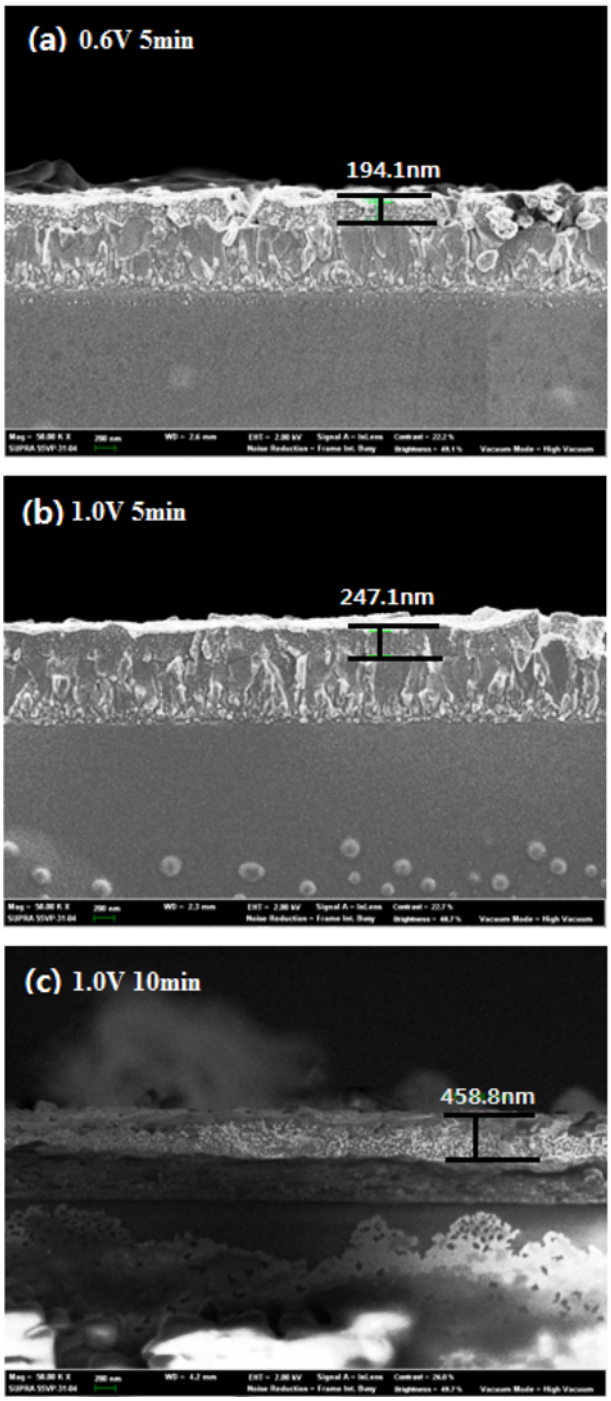


**Fig. 5. Cross-sectional SEM images of electrodeposited blocking layers with different film thicknesses.**

bination through the surface compared to the rough surfaces having many possible electron doors for passages.

## 5. Analysis of Electrical Properties

As shown in Fig. 6, the thickness of the blocking layer increases at high voltage and at high deposition time. In addition, light transmittance through this blocking layer decreases for thick films. Therefore, it is necessary to examine photocurrent-voltage characteristics of DSSC using the blocking layers deposited with different voltage and deposition time. Fig. 9(a) shows the conversion efficiency for

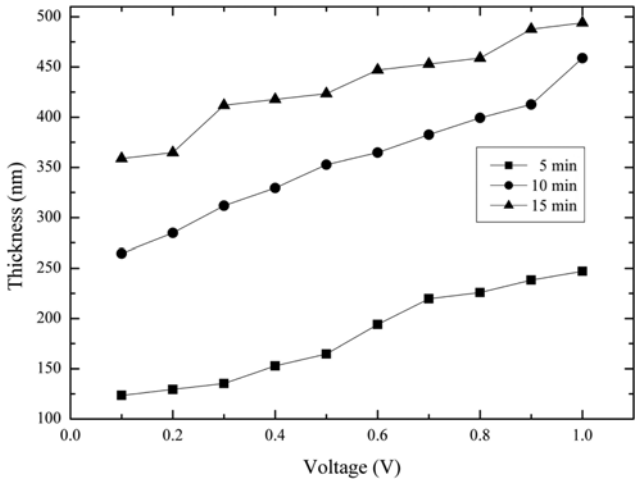


**Fig. 6. $TiO_2$ film thickness as a function of applied voltage for three deposition times.**

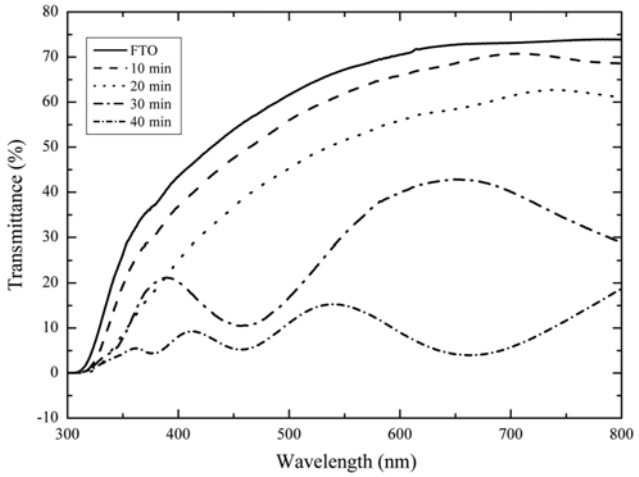


**Fig. 7. Transmittance spectra from the blocking layers fabricated at 0.7 V for various deposition times on FTO substrates.**

all experimental conditions, and it clearly shows the maximum values from the blocking layer fabricated at 0.7 V and incorporated into the DSSC. It is mainly attributed to the uniform and clean layer characteristics (no cracks) as explained in the SEM analysis. We further explored the conversion efficiency for thicker blocking layers which were deposited at 0.7 V for longer deposition time (Fig. 9(b)). The thickness of the blocking layer increases proportionally to the electrodeposition time, but the conversion efficiency shows high values for only the blocking layer thickness of 400 nm to 600 nm, with the maximum efficiency at about 450 nm. The reduction of the conversion efficiency for the thick blocking layer possibly results from the reduction of light transmittance, as discussed in UV-vis spectrophotometer analysis. Other articles [27,28] also reported the optimal thickness in DSSC for a blocking layer made from a sputtering method to be 400 nm to 450 nm, and it is consistent with this study.

Fig. 10(a) shows the comparison of photocurrent density-voltage (J-V) characteristics from the reference DSSC (no blocking layer) and from the DSSC with the blocking layer formed at 0.7 V for 20 min. The cell efficiency was improved about 59.34% from 2.41%

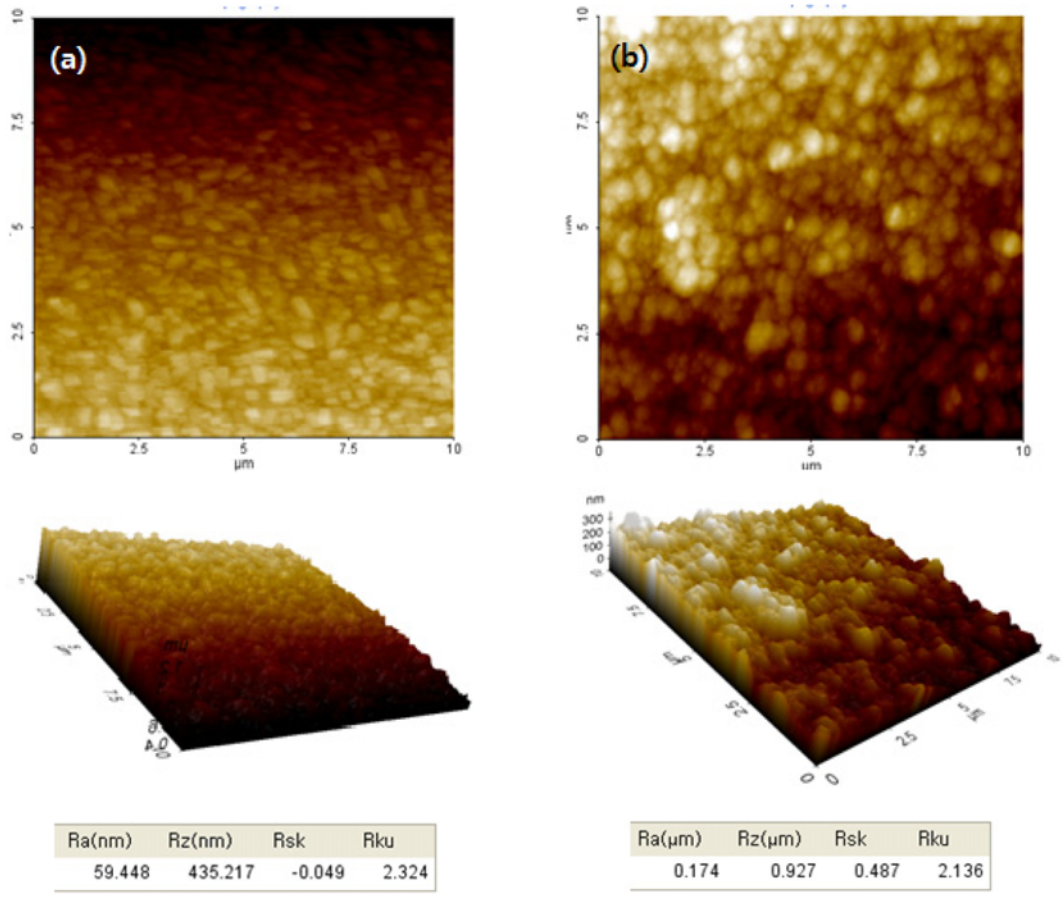


**Fig. 8. AFM images from (a) the blocking layer and from (b) a bare FTO glass.**

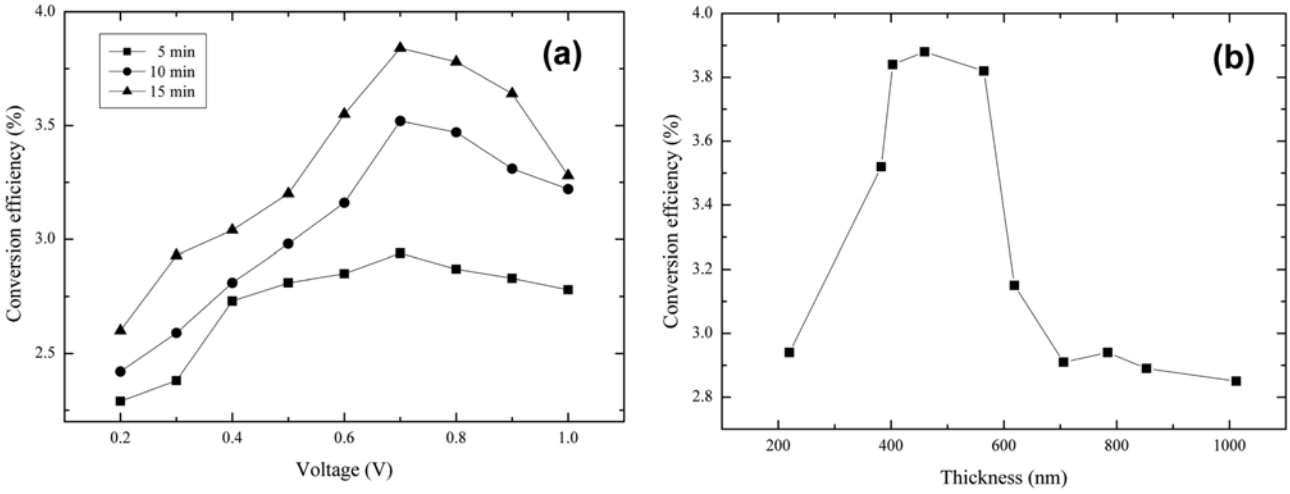


**Fig. 9. Conversion efficiency of DSSCs including various thicknesses of blocking layers made from different voltages and deposition times (a), and conversion efficiency of DSSCs as a function of thickness of blocking layer made at 0.7 V (b).**

to 3.84% by introducing the electrodeposited $TiO_2$ blocking layer. In addition, Fig. 10(b) demonstrates the dark current-voltage characteristic curve to see the effect of the blocking layer, and shows that the onset of the dark current occurs at high forward bias with the blocking layer due to suppressing the recombination reaction. It is attributed to the reduced electron recombination without much loss of light transmittance by introducing effectively the $TiO_2$ blocking layer between the FTO substrate and the $TiO_2$ paste film.

## CONCLUSIONS

A flat, dense, and compact $TiO_2$ nanocrystalline film on bare FTO

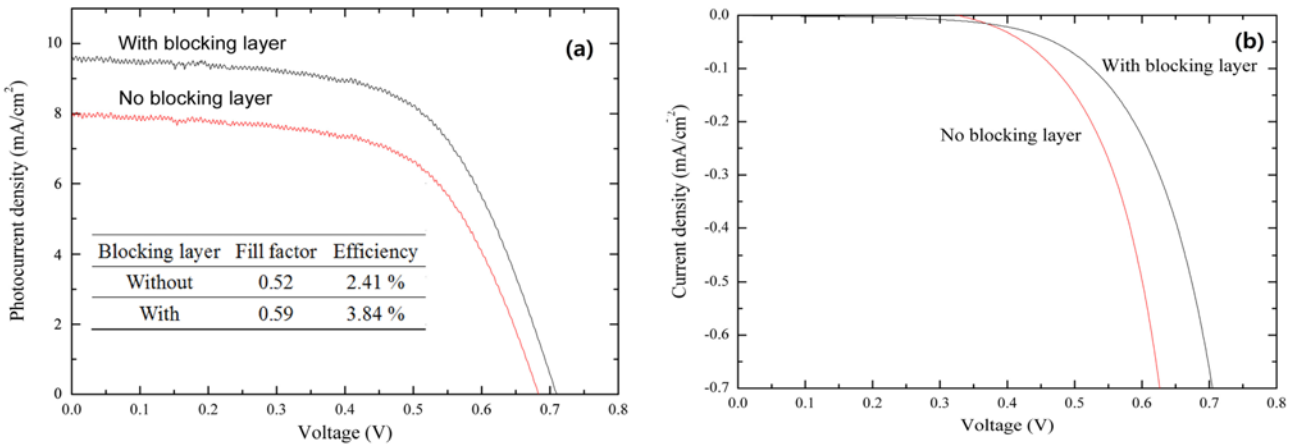


**Fig. 10. I-V curves of DSSCs for photocurrent (a) and dark current (b) densities from the cells with the blocking layer and no blocking layer.**

substrate was fabricated by electrodeposition method. The blocking layer has similar crystalline structure regardless of deposition time and applied voltage, and the layer thickness increases with increasing the deposition time and applied voltage. A clear boundary of the applied voltage for electrodeposition was observed for minimizing crack formation on the blocking layer. The optimum voltage and thickness in DSSC application with the blocking layer were found to be approximately 0.7 V and 450 nm. Applying this blocking layer to the DSSC, the cell efficiency was enhanced by 59.34% from 2.41% to 3.84%, compared to the reference cell case without the blocking layer.

## ACKNOWLEDGEMENT

This work was supported by the 2011 Research Fund of the University of Seoul.

## REFERENCES

1. S. W. Rhee and W. Kwon, *Korean J. Chem. Eng.*, **28**, 1481 (2011).
2. M. Gratzel, *J. Photochem. Photobiol. C: Photochemistry Reviews*, **4**, 145 (2003).
3. E. Hong, J. H. Kim and S. Yu, *Korean J. Chem. Eng.*, **28**, 1684 (2011).
4. D. J. Yang, S. C. Yang, J. M. Hong, H. Lee and I. D. Kim, *Journal of Electroceramics*, **24**, 200 (2010).
5. D. H. Lee, M. J. Lee, H. M. Song, B. J. Song, K. D. Seo, M. Pastore, C. Anselmi, S. Fantacci, F. De Angelis, M. K. Nazeeruddin, M. Gräetzel and H. K. Kim, *Dyes Pigm.*, **91**, 192 (2011).
6. B. Yoo, K. J. Kim, S. Y. Bang, M. J. Ko, K. Kim and N. G. Park, *J. Electroan. Chem.*, **638**, 161 (2010).
7. B. Bills, M. Shanmugam and M. F. Baroughi, *Thin Solid Films*, **519**, 7803 (2011).
8. E. Palomares, J. N. Clifford, S. A. Haque, T. Lutz and J. R. Durrant, *Journal of the American Chemical Society*, **125**, 475 (2003).
9. H. F. Wang, L. Y. Chen, W. N. Su, J. C. Chung and B. J. Hwang, *J. Phys. Chem. C*, **114**, 3185 (2010).
10. J. A. Jeong and H. K. Kim, *Solar Energy Materials and Solar Cells*, **5**, 64 (2010).
11. L. Meng and C. Li, *Nanosci. Nanotechnol. Letters*, **3**, 181 (2011).
12. K. Han and J. H. Kim, *Mater. Letters*, **65**, 2466 (2011).
13. S. J. Wang, Y. X. Xu, M. Ma and T. L. Fan, *Materials Science Forum*, **663**, 848 (2011)
14. P. J. Cameron and L. M. Peter, *J. Phys. Chem. B*, **107**, 14394 (2003).
15. S. Ito, P. Liska, P. Comte, R. Charvet, P. Pechy, U. Bach, L. Schmidt-Mende, S. M. Zakeeruddin, A. Kay, M. K. Nazeeruddin and M. Grätzel, *Chem. Commun.*, **34**, 4351 (2005).
16. C. Y. Kuo, S. Y. Lien, Z. S. Wu, F. S. Shieu and C. F. Chen, *Nanosci. Nanotechnol. Letters*, **3**, 195 (2011).
17. J. N. Hart, D. Menzies, Y. B. Cheng, G. P. Simon and L. Spiccia, *Comptes Rendus Chimie*, **9**, 622 (2006).
18. K. Wessels, M. Wark and T. Oekermann, *Electrochim. Acta*, **55**, 6352 (2010).
19. I. Mukhopadhyay, C. L. Aravinda, D. Borissov and W. Freyland, *Electrochim. Acta*, **50**, 1275 (2005).
20. C. C. Huang, H. C. Hsu, C. C. Hu, K. H. Chang and Y. F. Lee, *Electrochim. Acta*, **55**, 7028 (2010).
21. C. C. Hu, C. C. Huang and K. H. Chang, *Electrochem. Commun.*, **11**, 434 (2009).
22. C. D. Lokhande, B. O. Park, H. S. Park, K. D. Jung and O. S. Joo, *Ultramicroscopy*, **105**, 267 (2005).
23. C. Lokhande, S. K. Min, K. D. Jung and O. S. Joo, *J. Mater. Sci.*, **39**, 6607 (2004).
24. M. S. Wu, M. J. Wang, J. J. Jow, W. D. Yang, C. Y. Hsieh and H. M. Tsai, *J. Power Sources*, **185**, 1420 (2008).
25. E. Fatas, P. Herrasti, F. Arjona, E. G. Camarero and J. Medina, *Electrochim. Acta*, **32**, 139 (1987).
26. H. Chang, H. T. Su, W. A. Chen, K. David Huang, S. H. Chien, S. L. Chen and C. C. Chen, *Solar Energy*, **84**, 130 (2010).
27. M. Wu, Z. H. Yang, Y. H. Jiang, J. J. Zhang, S. Q. Liu and Y. M. Sun, *J. Solid State Electrochem.*, **14**, 857 (2010).
28. I. Seigo and K. Mohammad, *Int. J. Photoenergy*, **2009**, 8 (2009).